The EMBO Journal (2012) 31, 1231–1240 | © 2012 European Molecular Biology Organization | All Rights Reserved 0261-4189/12
www.embojournal.org

THE EMBO JOURNAL

Microvesicles released from microglia stimulate synaptic activity via enhanced sphingolipid metabolism

Flavia Antonucci[1], Elena Turola[1], Loredana Riganti[1], Matteo Caleo[2], Martina Gabrielli[1], Cristiana Perrotta[3], Luisa Novellino[1], Emilio Clementi[3,4], Paola Giussani[5], Paola Viani[5], Michela Matteoli[1,6] and Claudia Verderio[1,*]

[1]Department of Medical Pharmacology, CNR Institute of Neuroscience, Università di Milano, Milano, Italy, [2]CNR Institute of Neuroscience, Pisa, Italy, [3]Unit of Clinical Pharmacology, Department of Clinical Sciences, University Hospital Luigi Sacco, Università di Milano, Milano, Italy, [4]E-Medea Scientific Institute, Bosisio Parini (LC), Italy, [5]Department of Medical Chemistry, Biochemistry and Biotechnology, Laboratorio Interdisciplinare di Tecnologie Avanzate, Università di Milano, Segrate (Milan), Italy and [6]IRCCS Istituto Clinico Humanitas, Rozzano, Italy

Microvesicles (MVs) released into the brain microenvironment are emerging as a novel way of cell-to-cell communication. We have recently shown that microglia, the immune cells of the brain, shed MVs upon activation but their possible role in microglia-to-neuron communication has never been explored. To investigate whether MVs affect neurotransmission, we analysed spontaneous release of glutamate in neurons exposed to MVs and found a dose-dependent increase in miniature excitatory postsynaptic current (mEPSC) frequency without changes in mEPSC amplitude. Paired-pulse recording analysis of evoked neurotransmission showed that MVs mainly act at the presynaptic site, by increasing release probability. In line with the enhancement of excitatory transmission *in vitro*, injection of MVs into the rat visual cortex caused an acute increase in the amplitude of field potentials evoked by visual stimuli. Stimulation of synaptic activity occurred via enhanced sphingolipid metabolism. Indeed, MVs promoted ceramide and sphingosine production in neurons, while the increase of excitatory transmission induced by MVs was prevented by pharmacological or genetic inhibition of sphingosine synthesis. These data identify microglia-derived MVs as a new mechanism by which microglia influence synaptic activity and highlight the involvement of neuronal sphingosine in this microglia-to-neuron signalling pathway.

The EMBO Journal (2012) **31,** 1231–1240. doi:10.1038/emboj.2011.489; Published online 13 January 2012
Subject Categories: membranes & transport; neuroscience
Keywords: excitatory transmission; microglia; microvesicles; sphingosine

*Corresponding author: Department of Medical Pharmacology, CNR Institute of Neuroscience, Università di Milano, Via Vanvitelli 32, Milano 20129, Italy. Tel.: +39 02 50317098; Fax: +39 02 7490574; E-mail: c.verderio@in.cnr.it

Received: 21 June 2011; accepted: 7 December 2011; published online: 13 January 2012

Introduction

Despite microvesicles (MVs) were originally described as inert debris, their functional relevance has become now clear and MV shedding is a recognized mode of intercellular communication. MVs, also referred to as shed vesicles or ectosomes (Sadallah *et al*, 2011) are small (0.1–1 μm) membrane-bound vesicles that extrude from cells during activation. MVs contain surface proteins, cytoplasmic and nuclear material of parent cells and can transfer these components to target cells (Cocucci *et al*, 2009). MVs are believed to originate from lipid rafts and contain lipid rafts elements (Del Conde *et al*, 2005) together with bioactive lipids such as arachidonic acid and sphingosine-1-phosphate (S-1P) (Ratajczak *et al*, 2006; Thomas and Salter, 2010). In addition, it is well known that MVs lose membrane asymmetry and are characterized by externalization of phosphatidylserine (PS; Zwaal and Schroit, 1997; Sims and Wiedmer, 2001). PS exposed on shed MVs represents a determinant for recognition on recipient cells, through binding to the corresponding cellular PS receptors (Al-Nedawi *et al*, 2009). Besides receptor-ligand binding and endocytosis, the interaction of MVs with recipient cells can occur by fusion. Alternatively, MVs can undergo rupture and release luminal active components, thus modulating, by protein secretion, the activity of target cells.

We have recently shown that a specialized type of MV release exists for glial cells that express $P2X_7$ receptors, which shed MVs from the cell surface when exposed to ATP *in vitro*. MV production is controlled by acid sphingomyelinase (A-SMase), which hydrolyses membrane sphingomyelin (SM) to ceramide, the precursor of other bioactive sphingolipids. During ATP activation, A-SMase moves to plasma membrane outer leaflet, where it induces MV budding, and remains associated with shed MVs (Bianco *et al*, 2009b). MVs shed from glial cells and brain tumour store the pro-inflammatory cytokine IL-1β (Bianco *et al*, 2005), angiogenic factors and their respective mRNAs, and matrix metalloproteinases (Al-Nedawi *et al*, 2008; Proia *et al*, 2008; Sbai *et al*, 2010). These factors are released by glial cells also through a distinct type of vesicles, exosomes (Skog *et al*, 2008; Bianco *et al*, 2009b), smaller and more homogeneous organelles, which result from the exocytosis of multivesicular bodies, and which are released under the control of neutral sphingomyelinase (Trajkovic *et al*, 2008; Kosaka *et al*, 2010). Exciting evidence indicate that both shed MVs and exosomes derived from glial tumours are taken up by brain endothelial cells and gain access to compartments external to the CNS, suggesting a role of these organelles in long range signalling (Al-Nedawi *et al*, 2008, 2009; Skog *et al*, 2008; Graner *et al*, 2009). By contrast, little information is available about the physiological role of MVs derived from non-tumour glial cells in short range intercellular communication within the brain (van der Vos *et al*, 2011).

Given inflammatory mediators which affect glutamate transmission (Viviani *et al*, 2007; Vezzani *et al*, 2008) are stored within MVs and elements of the sphingolipids system, which also influence neurotransmitter release (Darios *et al*, 2009; Okada *et al*, 2009; Kanno *et al*, 2010; Norman *et al*, 2010), are localized at MV surface (Ratajczak *et al*, 2006; Bianco *et al*, 2009b), in this study we explored the possibility that MVs shed from glial cells upon $P2X_7$ receptors activation modulate neurotransmission. Functional $P2X_7$ receptors, active on A-SMase, and triggering MV shedding are expressed in almost all microglial cells in both culture and *in vivo* whereas in astrocytes the receptor expression is brain region specific (Bianco *et al*, 2009a) and its functional presence *in situ* is still controversial (Jabs *et al*, 2007). We therefore focused on MVs derived from microglial cells and found that they significantly enhance excitatory transmission, thus identifying MVs as a new pathway of microglia-to-neuron signalling.

Results

Microglia-derived MVs increase mEPSCs frequency and EPSC amplitudes

To evaluate whether microglia-derived MVs modulate synaptic transmission, we first analysed miniature excitatory postsynaptic currents (mEPSCs) in 14-day-old cultured hippocampal neurons, preexposed for 30–45 min to MVs produced either from primary microglia (Figure 1A–E) or from the N9 microglia cell line (Figure 3A). Given microglia are about as common as neurons in rodent brain but proliferate upon pathological alterations (Graeber, 2010), neurons were exposed to different amounts of MVs, produced by primary cells in a microglia-to-neuron relative ratio ranging from 1:1 to 4:1. A small increase in mEPSC frequency, which however did not reach a statistically significant difference, was evoked by MVs produced by microglia in a 1:1 ratio (1.2 μg/ml, obtained diluting in 600 μl of medium the MVs produced by 1.7×10^5 cells) while MVs produced by twice as many microglia as neurons increased the frequency of mEPSCs by more than two-fold (Figure 1B). The increase in mEPSC frequency was not associated with amplitude changes (Figure 1C), thus suggesting a presynaptic effect. Exposure to MVs also induced a small but significant increase in mEPSC decay (Figure 1E), but not rise time (Figure 1D), suggesting a mild effect of MVs on the gating of postsynaptic receptors. A higher concentration of MVs, produced by donor cells in a microglia-to-neuron ratio of 4:1 caused a stronger stimulation of mEPSC frequency (Figure 1B) but also tended to increase the current noise. Therefore, a microglia-to-neuron ratio of 2:1 was utilized in subsequent experiments.

Evaluation of neuronal availability by calcium imaging recordings and annexin-V staining ruled out any acute or delayed toxic effects mediated by microglia-derived MVs (Supplementary Figure S1). Monitoring vesicle exocytosis under depolarized conditions (50 mM KCl, 4 min) using antibodies directed against the luminal domain of synaptotagmin I (Syt-ECTO Ab) (Matteoli *et al*, 1992), revealed that exposure to MVs induced a small but significant increase in the fraction of glutamatergic boutons positive for Syt-ECTO Ab ($N = 5$; percentage of recycling synapses, Ctr $= 100 \pm 3.5$; MV-treated neurons $= 112.9 \pm 4.9$, *t*-test followed by Mann–Whitney rank-sum test, $P = 0.04$), suggesting an increase in synaptic vesicle recycling. Consistent with these data, paired recordings of neurons exposed to MVs showed a larger amplitude of evoked EPSCs as compared with controls (Figure 1F and G). To evaluate whether the enhanced EPSC amplitude results from an increase in release probability, we measured short-term plasticity, by recording from pairs of neurons at 50 ms interval. While paired-pulse facilitation (PPF) usually occurs in control cultures (Figure 1H), synaptic connections showed paired-pulse depression (PPD) in MV-treated cultures, indicating an increase in release probability (10 sweeps-trial/pairs; Figure 1H–I). To address whether the switch from PPF to PPD could result from a change in the size of the ready releasable pool (RRP) of vesicles, which are docked and primed for fusion, we analyse sucrose-evoked exocytosis, which reflects the calcium-independent release of the RRP (Rosenmund and Stevens, 1996). A 4-s long local application of hypertonic solution to synaptic regions produced larger bursts of quantal events in neurons exposed to MVs, indicating a larger RRP of vesicles (Figure 1J–L). Altogether, these results indicate that a larger RRP of vesicles, together with an increase in release probability, account for the enhanced amplitude of EPSCs induced by MVs.

MVs enhance the amplitude of evoked responses in vivo

To address whether MVs stimulate evoked transmission *in vivo*, visual evoked potentials (VEPs) were recorded in rats, before and 1 h after MVs injection into primary visual cortex. VEPs represent the integrated synaptic response of cortical cells to visual stimulation and reflect the sum of excitatory currents elicited by the sensory stimulus (Porciatti *et al*, 1999; Restani *et al*, 2009). We found that injection of control, saline solution, had no effect on VEP amplitudes (Figure 2A). Conversely, field potential responses were significantly potentiated by MVs injection (1.5 μg/μl; Figure 2B). In particular, a consistent enhancement was found for responses to high contrast stimuli (90% contrast; Figure 2B). Latency of VEPs was not impacted by either saline or MV delivery (Figure 2C). Analysis of the spiking activity of single cortical units revealed a significant enlargement of neuron receptive fields (RFs) after MV, but not saline, injection (Figure 2D). An increase in RF size is consistent with the enhancement of excitatory synaptic transmission in visual cortex (Benali *et al*, 2008).

The stimulatory activity of MVs requires interaction of MVs with neuronal surface and does not depend on cytokines

To verify whether interaction of MVs with the plasma membrane of neurons is required for the stimulatory action, MVs were pretreated with annexin-V, which prevents binding of PS, externalized on MVs, to corresponding neuronal receptors. Cloaking PS significantly reduced MV-induced increase of mEPSC frequency, suggesting that the interaction between MVs and neurons is relevant for the biological effect (Figure 3A). No changes were observed in mEPSC activity after incubation of neurons with annexin-V alone.

The inflammatory mediators TNF-α and IL-1β are among the proteins contained in MVs shed from reactive microglia (Bianco *et al*, 2005), which can contribute to modulate neuronal activity. Since TNF-α and IL-1β synthesis is upregulated in response to inflammatory stimuli (Akira and Takeda, 2004; Thomas and Salter, 2010), to highlight the

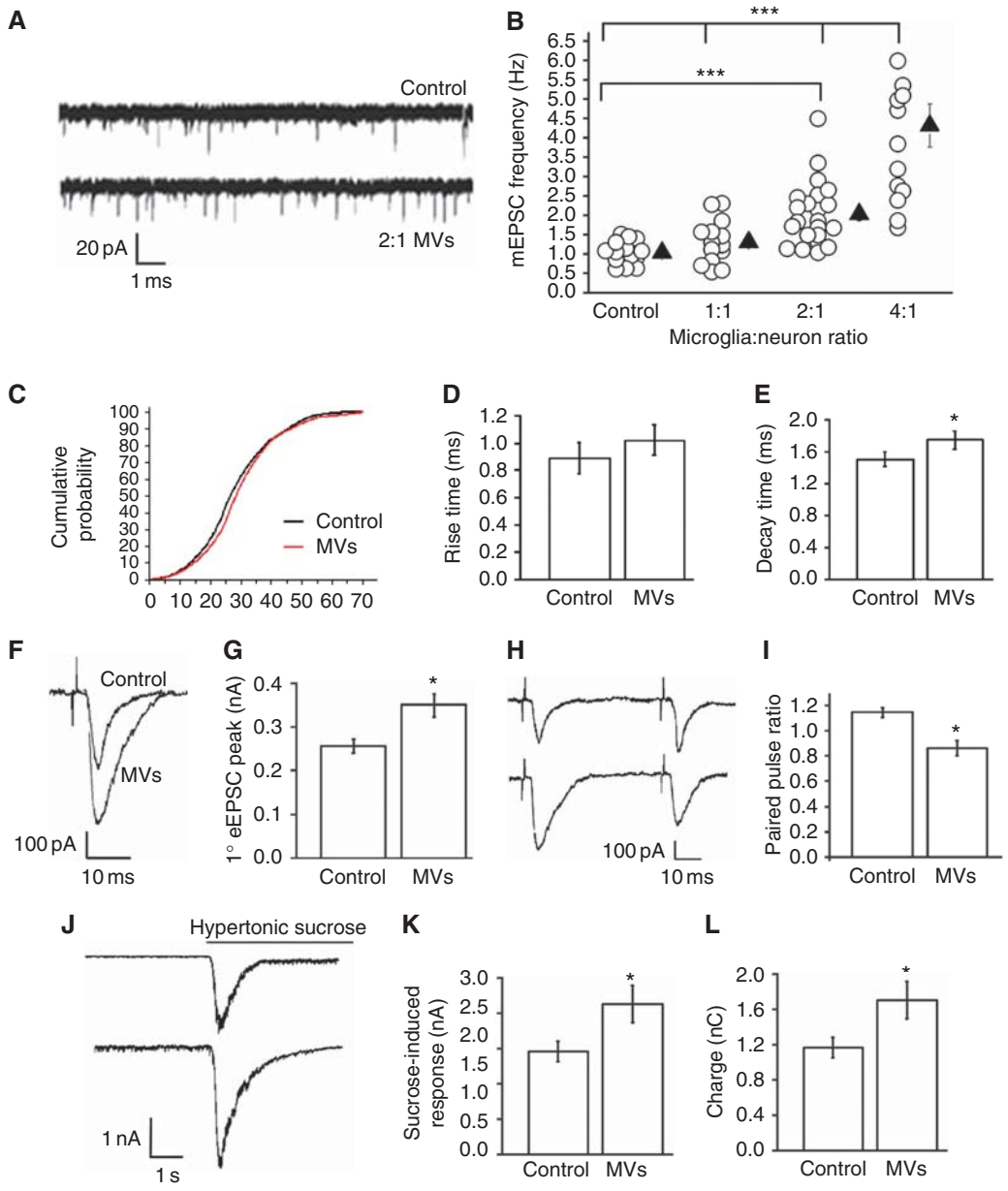

Figure 1 Effect of MVs on neurotransmission in hippocampal cultures. (**A**) Representative traces of mEPSCs from control neurons and neurons exposed to MVs. (**B**) Changes of mEPSC frequency evoked by MVs in a microglia-to-neuron ratio of 1:1 (MVs concentration = 1.2 μg/ml), 2:1 (MVs concentration = 2.38 μg/ml), and 4:1 (MVs concentration = 4.76 μg/ml); $N = 3$; one-way ANOVA followed by Dunn's method, $P < 0.001$. (**C**) Cumulative distribution of mEPSC amplitude from control and MV-treated neurons; $n = 15$ controls; $n = 12$ MV-treated neurons; *t*-test followed by Mann–Whitney, $P = 0.054$. (**D**, **E**) Rise time (**D**), *t*-test followed by Mann–Whitney rank-sum test, $P = 0.071$ and decay time (**E**), $n = 10$ controls; $n = 15$ MV-treated neurons; test followed by Mann–Whitney, $P = 0.006$ of mEPSCs from control and MV-treated neurons. (**F**, **G**) Examples of stimulus-evoked EPSCs in control and MV-treated paired mouse neurons (**F**) and corresponding mean amplitude (**G**); *t*-test $P = 0.001$, $N = 3$, 11 versus 10 pairs, respectively. (**H**, **I**) Representative traces of short-term plasticity in paired mouse neurons (**H**) and quantitative analysis of paired-pulse ratio (**I**); $n = 10$ pairs per conditions, $N = 3$, *t*-test followed by Mann–Whitney rank-sum test, $P = < 0.001$. (**J**) Representative sucrose-evoked responses from control and MV-treated neurons. (**K**, **L**) Mean amplitude (nA) and total charge (pC) of sucrose-evoked responses; $N = 4$, $n = 16$ Ctr; $n = 24$ MV-treated cells; current (nA), *t*-test followed by Mann–Whitney rank-sum test, $P = 0.025$; charge transferred (nC), $P = 0.042$.

possible involvement of cytokines we evaluated the effects of MVs produced by cells activated with LPS. A similar increase in mEPSC frequency (Figure 3B) but not mEPSC amplitude (Figure 3C) was induced by MVs produced by LPS-treated microglia as compared with MVs derived from resting microglia. Furthermore, no reduction of mEPSC frequency (Figure 3B) or decay time (Ctr = 1.508 ± 0.09 ms, $n = 10$ cells; MVs treated = 1.748 ± 0.10 ms, $n = 8$, LPS-MVs treated 1.83 ± 0.086 ms, $n = 7$; MVs treated + neutrAb 1.87 ± 0.13 ms, $n = 7$ and LPS-MVs treated + neutrAb = 1.73 ± 0.15 ms, $n = 5$; LPS-MVs treated versus LPS-MVs treated + neutrAb, *t*-test followed by Mann–Whitney rank-sum test, $P = 0.0917$) was observed in neurons exposed to MVs in the presence of TNF-α and IL-1β neutralizing antibodies. Altogether, these data suggest that the enhancement of exocytosis induced by MVs does not depend on the release of TNF-α and IL-1β from MVs,

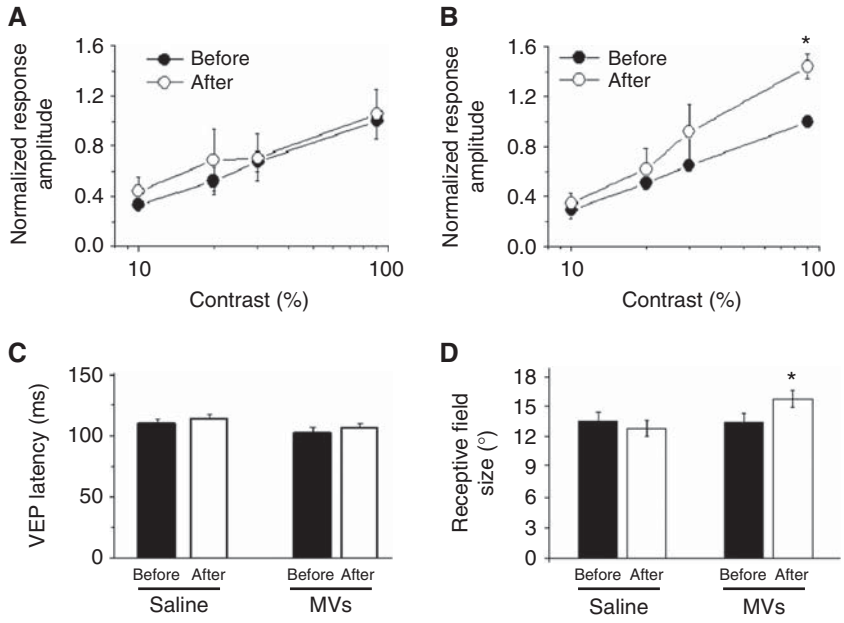

Figure 2 MVs increase field potential responses *in vivo*. (**A**, **B**) Contrast threshold curves obtained before and after delivery of saline (**A**, $n=4$ rats; two-way repeated measures ANOVA, baseline versus post saline, $P=0.84$) or MVs (**B**, $n=6$ rats) into the visual cortex. The VEP amplitude for each contrast value is normalized to the amplitude of the response at contrast = 90% before injection. Note the significant potentiation of the VEP response to 90% contrast gratings following MVs (two-way repeated measures ANOVA followed by Holm–Sidak test, $P<0.05$). (**C**) VEP latencies before/after delivery of saline or MVs. Latency of visual response is not affected (paired *t*-test, $P>0.49$ for all comparisons) by either treatment. (**D**) RF sizes before/after delivery of saline or MVs. Note the significant enlargement of RFs following MVs injection (paired *t*-test, $P<0.05$), but not after saline injection (paired *t*-test; MVs, $P=0.015$ and saline, $P=0.68$, respectively). Before saline, $n=30$ cells; after saline $n=28$ cells; before MVs, $n=42$ cells; after MVs, $n=38$ cells.

consistent with the low levels of these cytokines in MVs derived from unstimulated cells.

Surface components of MVs mediate stimulation of exocytosis

To investigate whether the effects of MVs were mediated by factor/s present at the surface or in the lumen of these organelles, MVs were broken by freeze and thaw, pelleted to remove soluble components and then added to cultured neurons. Figure 3D shows that broken vesicles, depleted of their content, retained the capability to increase frequency of mEPSCs, indicating that surface component/s were sufficient to stimulate exocytosis. Freeze and thaw MV disruption was assessed by detection of IL-1β release from MVs produced by LPS-primed microglia (Figure 3E) and by flow cytometry analysis of MVs shed from microglia loaded with the calcein analogue CMFDA (Figure 3F). Higher levels of soluble IL-1β were detected in the medium containing MVs subjected to freeze and thaw as compared with intact MVs (Figure 3E). Accordingly, whereas intact MVs that retained CMFDA within the MV cytoplasm displayed a fluorescent signal, a strong reduction in CMFDA fluorescence was detected in MVs subjected to freeze and thaw (Figure 3F). To get insights into the possible role of MVs lipids, neurons were exposed to synthetic liposomes, similar in size to MVs, having PS externalized and mimicking the phospholipid composition of the plasma membrane (60% PC, 20% cholesterol, 10% SM, 10% PS). No increase in mEPSC frequency was detected in cultures incubated with liposomes, excluding a major involvement of the main phospholipid constituents of the plasma membrane, including externalized PS, in the biological effect of MVs (Figure 3G). However, the lipid fraction extracted from MVs was able to increase mEPSC frequency at an extent similar to that of intact MVs (Figure 3G). Therefore, this indicates that the stimulatory agent is associated with the MV lipid component.

Microglia-derived MVs increase sphingolipid metabolism

Recent evidence indicates that the sphingolipids sphingosine (Sph) and its metabolite sphingosine-1P (S-1P) facilitate transmitter release from synaptic terminals (Darios *et al*, 2009; Okada *et al*, 2009; Kanno *et al*, 2010; Norman *et al*, 2010). Sph can be produced from SM by sequential activity of SMase and ceramidase, and converted by sphingosine kinase to S-1P. This prompted us to investigate whether MVs may facilitate sphingolipid availability in neurons and enhance therefore exocytosis.

We first evaluated sphingolipid metabolism in neurons, exposed or not to MVs, after labelling cells with [Sph-3H]SM. In control and MV-treated neurons, the amount of cell-associated radioactivity was very similar. The incubation with MVs promoted a significant increase of 3H ceramide and 3H Sph with a concomitant decrease of 3H-SM (Figure 4A), thus indicating that MVs actually stimulate 3H-SM breakdown in neurons. Application of exogenous A-SMase, as well as SM metabolite Sph and its phosphoderivative S-1P all mimicked the stimulation of mEPSC frequency induced by MVs (Figure 4B). A-SMase (2 U/ml), Sph (1 μM), and S-1P (1 μM) increased the frequency of mEPSC by 1.96-, 1.84-, and 2.7-fold, respectively. No changes in mEPSC amplitude were induced by either Sph or S-1P

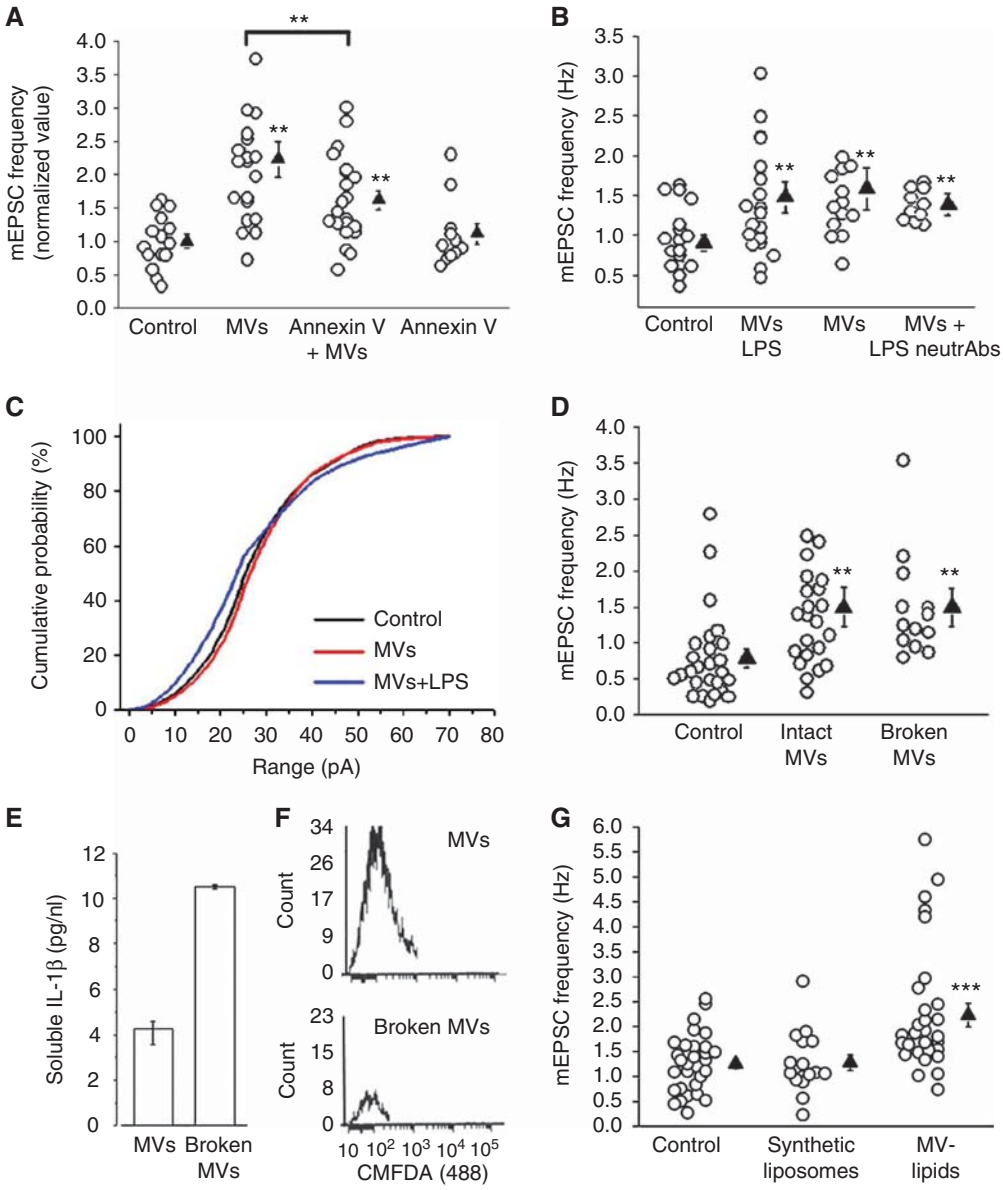

Figure 3 Surface components of MVs stimulate of exocytosis. (**A**) Normalized mEPSC frequency of control neurons and neurons exposed to MVs pretreated with annexin-V; $N=3$, one-way ANOVA followed by Fisher's LSD methods, $P<0.001$. (**B**) mEPSC frequency of control neurons and neurons exposed to MVs derived from resting or LPS-primed microglia with or without TNF-α and IL-1β neutralizing Abs; $N=3$, one-way ANOVA followed by Dunn's test, $P=0.003$, LPS-MV-treated versus LPS-MVs-treated + neutrAb *t*-test, $P=0.439$. (**C**) Cumulative distribution of mEPSC amplitudes as in (**B**). (**D**) mEPSC frequency from control neurons, neurons exposed to intact or empty N9-MVs, broken by freeze and thaw; $N=3$, one-way ANOVA followed by Dunn's test, $P=0.002$. (**E**) MVs shed from LPS-primed N9 in saline were subjected or not to freeze and thaw. The histogram shows the concentration of IL-1β detected by ELISA in the saline containing intact MVs or broken MVs. (**F**) Flow cytometry plots for CMFDA of intact and broken MVs. (**G**) Rate of mEPSCs recorded from control neurons and neurons exposed to either artificial liposomes or native lipids from MVs; $N=3$, one-way ANOVA followed by Dunn's methods, $P=0.002$.

(Ctr = −44.11 ± 2.79 pA, Sph treated = −47.13 ± 1.46 pA, S-1P treated = −43.13 pA), but Sph significantly increased the decay time (Ctr = 1.50 ± 0.095 ms; Sph treated = 1.88 ± 0.12 ms, *t*-test followed by Mann–Whitney rank-sum test, $P<0.001$). We then evaluated whether pretreatment of neurons with the ceramidase inhibitor *N*-oleoylethanolamine (NOE; Strelow *et al*, 2000), to prevent metabolism of ceramide to Sph, or with the Sph kinase inhibitor SKI-1, to prevent metabolism of Sph to S-1P (Kanno *et al*, 2010), impaired the stimulatory action of MVs. Pretreatment of neurons with 37 μM NOE but not with 2 μM SKI-1 strongly inhibited the increase in mEPSCs frequency induced by MVs (Figure 4C). No changes were observed in mEPSC frequency after incubation of neurons with NOE or with SKI-1 alone (NOE treated = 0.67 ± 0.08 Hz, $n=8$ cells; SKI-1 treated = 0.81 ± 0.12 Hz, $n=8$ cells). These data indicate that the biological activity of MVs requires sphingolipid metabolism in neurons and indicate Sph as the key sphingolipid involved in the enhancement of excitatory neurotransmission.

Neuronal A-SMase mediates MV-induced facilitation of exocytosis

To investigate the contribution of A-SMase to sphingolipid metabolism and increased mEPSC frequency, neurons established from A-SMase KO mice were exposed to MVs. A-SMase

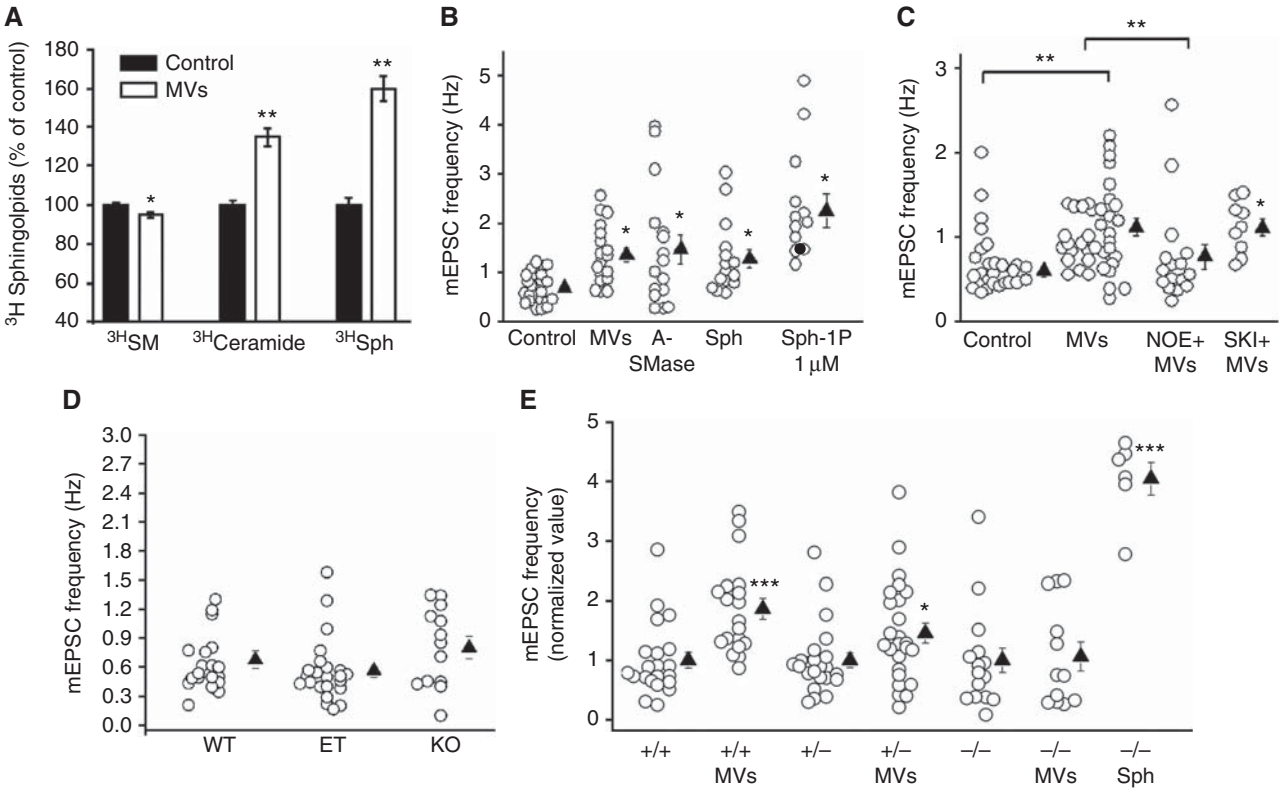

Figure 4 MVs stimulate sphingolipid synthesis in neurons. (**A**) A-SMase activity of MVs and of donor N9 cells. Values were normalized to protein concentration of equivalent amounts of MVs and N9. Cells were pulsed 1 h with [Sph-3H]SM followed by 1 h chase with or without MVs. Cell lipids were extracted and analysed as described in Supplementary data. Data are expressed as % of control. (**B**) Neurons were exposed to bacterial A-SMase (2 U), Sph (1 μM) or S-1P (1 μM) for 30 min, washed and mEPSCs were recorded for the subsequent 45 min. The graph shows mEPSC frequency under above conditions; $N=3$ for A-SMase and Sph, $N=2$ for S-1P; one-way ANOVA followed by Fisher's methods, $P=0.014$. (**C**) Rate of mEPSCs of control and MV-treated neurons with or without NOE and SKI-1; $N=3$; Ctr versus MVs treated, one-way ANOVA followed by Fisher's methods, $P<0.001$. (**D**) Rate of mEPSCs of hippocampal neurons established from WT, heterozygous or A-SMase KO mice; $N=3$, Kruskal–Wallis one-way ANOVA on ranks, $P=0.085$. (**E**) mEPSC frequency (normalized data) of WT, heterozygous and KO A-SMase neurons exposed or not to MVs produced by primary microglia or Sph (1 μM); $N=3$, $^{+/+}$A-SMase versus $^{+/+}$A-SMase + MVs: *t*-test followed by Mann–Whitney rank-sum test, $P<0.001$; $^{+/-}$A-SMase versus $^{+/-}$A-SMase + MVs *t*-test followed by Mann—Whitney, $P=0.026$; $^{-/-}$A-SMase versus $^{-/-}$A-SMase + MVs: *t*-test, $P=0.981$.

KO neurons did not display significant alteration of mEPSC frequency as compared with heterozygous or wild-type neurons (Figure 4D), consistent with normal basal synaptic transmission (Camoletto *et al*, 2009). As expected, exposure of WT neurons to MVs increased the frequency of mEPSCs (Figure 4E). Conversely, reduced stimulation of mEPSC frequency was observed in A-SMase heterozygous neurons and no increase in the rate of mEPSCs was detected in A-SMase KO neurons (Figure 4E). A significant increase of mEPSCs frequency was observed in response to externally added Sph (1 μM) in A-SMase KO neurons, thus excluding that accumulation of SM at the synaptic membranes of A-SMase knockout neurons (Camoletto *et al*, 2009) may hide the stimulatory action of MVs. Data obtained in A-SMase KO neurons suggest that neuronal A-SMase is the enzyme responsible for the increased metabolism of sphingolipids and facilitation of excitatory transmission caused by MVs. Furthermore, these results exclude that MVs stimulate exocytosis by directly transferring bioactive sphingolipids to neuronal terminals.

Discussion

In the present study, we unveiled a novel mechanism by which microglia can modulate neuronal activity. MVs shed from the surface of microglia interact with the plasma membrane of neurons and enhance spontaneous and evoked excitatory transmission, without producing any acute or delayed neurotoxic effects. Of note, evaluation of neuronal availability by calcium imaging recordings and annexin-V staining in neuronal cultures exposed up to 5 days to MVs, rule out any acute or delayed neurotoxic effects of MVs. The minimal amount of MVs needed to elicit a significant stimulation of neurotransmission is that produced by twice as many cultured microglial cells as recipient neurons, in a microglia-to-neuron ratio not distant from the 1:1 value occurring in brain (Graeber, 2010). A similar increase in mEPSC frequency is induced by MVs derived from cultured astrocytes, when diluted in the culture medium up to the minimal active concentration determined for microglial MVs (2.4 μg/ml) (Supplementary Figure S2). However, vesiculation is less efficient in cultured astrocytes than in microglia, suggesting a lower potential of MVs of astrocytic origin in modulating neuronal exocytosis.

MVs mainly act on the presynaptic site of the excitatory synapse, by increasing the RRP of vesicles and enhancing release probability at hippocampal synapses in primary cultures. We demonstrate that MVs influence neurotransmission by inducing sphingolipid metabolism in neurons.

Growing evidence suggests that SM metabolites, generated by SMase and ceramidase, regulate exocytosis and have functions beyond their structural role (Davletov and Montecucco, 2010). SMase and ceramidase activities have been linked to neurotransmitter release (Davletov and Montecucco, 2010) and the Sph metabolite S-1P has been reported to upregulate glutamate secretion in cultures (Kajimoto *et al*, 2007) and to increase action potential firing in CA1 neurons (Norman *et al*, 2010). Recently, it has been clarified that Sph, but not ceramide or S-1P, activates VAMP-2 to form SNARE fusion complexes, thus leading to enhanced mEPSC frequency, higher EPSC amplitude and larger RRP size (Darios *et al*, 2009). Our direct measurement of SM metabolism shows that MVs increase the breakdown of neuronal SM to ceramide and Sph. Experiments performed in A-SMase KO neurons suggest that the enzyme A-SMase is responsible for the first step of sphingolipid synthesis. In addition, results obtained using the ceramidase inhibitor NOE indicate that Sph production from ceramide is required for the presynaptic action of MVs. Of note, exposure to MVs produces exactly the same presynaptic changes induced by externally added A-SMase or Sph, that is, increase in mEPSC frequency but not amplitude, larger evoked EPSCs and sucrose-evoked responses and small but significant increase in mEPSC decay (Darios *et al*, 2009), suggesting a crucial role for Sph in stimulating exocytosis. Consistent with previous finding (Kanno *et al*, 2010) exogenously added S-1P also caused a strong stimulation of mEPSC frequency, without affecting their amplitude, suggesting that further metabolism of Sph to S-1P, by Sph kinase can contribute to enhanced neurotransmission. However, inhibition of Sph phosphorylation did not impair the MV-induced increase in mEPSC frequency, ruling out a major role of S-1P in the facilitation of exocytosis. These data do not exclude, however, that S-1P may contribute to the presynaptic action of MVs, through the involvement of molecular targets other than VAMP-2 in the complex array of molecules controlling exocytosis (Kajimoto *et al*, 2007; Darios *et al*, 2009).

The stimulatory effect of MVs requires MV interaction with the neuronal surface. Indeed, the increase in mEPSCs is reduced when the binding of externalized PS to its neuronal receptors is prevented by cloaking the phospholipid with annexin-V. Consistent with this finding, confocal analysis of hippocampal neurons exposed to GFP-labelled MVs, extensively washed and processed for immunocytochemistry, revealed the presence of few MVs anchored to the surface of neuronal processes (Supplementary Figure S3). The use of empty MVs, depleted of their luminal content, indicates that the presynaptic effect of MVs depends on surface components. Accordingly, MVs affect presynaptic functionality independently from the activation state, resting or reactive, of their parental microglia, as well as from the content of inflammatory cytokines and the presence of cytokine neutralizing antibodies. It has been recently shown that phospholipids present on the membrane of MVs mediate the biological activity of MVs derived from macrophages, which propagate an inflammatory signal among peripheral immune cells (Thomas and Salter, 2010). Accordingly, we found that the lipid fraction of MVs shed *in vitro* from microglia is responsible for their stimulatory capacity; however, the main phospholipid constituents of the plasma membrane, including PS, are not *per se* sufficient to activate neuronal SMase and sphingolipid metabolism in neurons, although PS externalized on MVs might facilitate MV recognition. Data obtained in A-SMase KO neurons suggest the requirement of neuronal A-SMase activity for enhancement of excitatory transmission and exclude that presynaptic stimulation depends on direct transfer of sphingolipids from MVs to neurons. However, we cannot exclude that lysosomal accumulation of SM and gangliosides in A-SMase KO neurons, by altering traffic along the endocytic pathway and plasma membrane organization of lipid rafts (Camoletto *et al*, 2009; Ledesma *et al*, 2011), may impair interaction of MVs with neurons and/or cell signalling leading to altered sphingolipid metabolism. Additional studies are required to identify the active lipid components of MVs, which are involved in the MV-evoked presynaptic stimulation.

Previous evidence indicates that MV release is induced by ATP, a physiological gliotransmitter (Verderio and Matteoli, 2001) but also a danger signal and that the shedding process occurs more efficiently in activated as compared with resting cells (Bianco *et al*, 2009b; Qu *et al*, 2009; Sarkar *et al*, 2009). Considering that the extracellular space is very limited in the CNS, it is likely that neurons *in vivo* may be exposed to active MV concentrations, especially in brain pathology, when ATP level raises in the extracellular space and microglial cells are promptly activated. By VEP and single unit recordings, we have here provided proof-of-principle that MVs can acutely alter excitatory synaptic transmission also *in vivo*. This was indicated by the significant enhancement of VEP amplitudes, which reflect the sum of excitatory currents elicited by visual stimulation (Porciatti *et al*, 1999; Restani *et al*, 2009), and by the increase in the RF size of cortical cells, which can be typically explained by an alteration of the excitation/inhibition balance in visual cortex (Benali *et al*, 2008; Liu *et al*, 2010). It is important to mention that these results were obtained with a high MV dose (1.5 μg/μl), and it is difficult to relate this dose to the potential amount of MVs that can be released *in vivo* under normal or pathological conditions. Thus, the relevance of the high MV dose employed remains to be established.

Uncontrolled microglial stimulation was previously linked to neurotoxicity and to a wide range of brain diseases. However, microglial reaction also supports neurons by providing trophic factors, eliminating damaged cells (Olah *et al*, 2011), controlling synaptogenesis (Roumier *et al*, 2004), and monitoring the functional state of synapses (Wake *et al*, 2009). Although we cannot exclude that MV-induced facilitation of exocytosis may represent a protective response of microglia, aimed at restoring neuronal activity upon functional deficit of synaptic transmission, it is more likely that MVs impact neurotransmission in case of microglia overshooting. By causing overproduction of sphingolipids, MVs shed from reactive microglia may contribute to the excessive potentiation of excitatory transmission, which occurs in neuroinflammatory and degenerative diseases (De Felice *et al*, 2007; Busche *et al*, 2008; Centonze *et al*, 2009). Consistent with this hypothesis, our unpublished data indicate that the amount of MVs produced *in vivo* by microglia, which can be recovered in the cerebrospinal fluid of rodents and humans, strongly increases under brain inflammation (Verderio C and Furlan R, unpublished observation). The present identification of lipids present on the MV surface as factors involved in the acute stimulation of presynaptic

activity does not rule out that cytokines stored inside MVs can enhance neurotransmission further, on a longer time scale, after being released from MVs.

Over the last years, MVs have gained increasing attention as an unconventional mechanism of intercellular communication within the brain but no evidence has been provided so far about their possible role in the modulation of neuron functionality by glial cells. Our data indicate that, among the variety of surface receptors and soluble factors which mediate the bidirectional communication between microglia and neurons (Ransohoff and Cardona, 2010; Olah *et al*, 2011), shed MVs represent a new mechanism by which microglia influence synaptic activity.

Materials and methods

Animal experiments

Long-Evans rats aged P26–P30 were used for VEP experiments. All efforts were made to minimize animal suffering and to reduce the number of animals used, in accordance with the European Communities Council Directive of 24 November 1986 (86/609/EEC).

Cell cultures

N9 microglia and microglia cultures P1 Sprague Dawley rats were obtained and maintained as described (Bianco *et al*, 2005). Rat or mouse hippocampal neurons were established from E18 fetal Sprague Dawley rats and from E18 embryonic A-SMase KO or WT littermate C57BL/6 mice (Horinouchi *et al*, 1995). The dissociated cells were plated onto poly-L-lysine-treated coverslips and maintained in Neurobasal with 2% B27.

MVs isolation

MVs shed upon exposure to BzATP (100 μM) for 30 min in Krebs-Ringer solution (125 mM NaCl, 5 mM KCl, 1.2 mM $MgSO_4$, 1.2 mM KH_2PO, 2 mM $CaCl_2$, 6 mM D-glucose, and 25 mM HEPES/NaOH, pH 7.4) were pelletted at 10 000 *g* for 30 min, as described previously (Bianco *et al*, 2009b). We obtained 4.2 ± 0.15 μg of MVs ($n = 5$, ± s.e.) from 1×10^6 primary microglia or from 5×10^6 N9 cells. Micro BCA protein assay kit (Thermo Fischer Scientific) was used to determine the protein concentration, according to the manufacturer's specifications. In all, 1.7×10^5 neurons were incubated with an amount of MVs (1.42 μg) produced by primary microglia in a microglia-to-neuron ratio of 2:1 for 30–45 min at 37°C if not otherwise stated, corresponding to an MV protein concentration of 2.38 μg/ml, obtained diluting MVs in 600 μl of medium. In case of MVs derived from N9 microglia, microglia-to-neuron ratio was 5:1. MVs were used immediately after isolation and never stored for later use. Shed MVs were broken by freeze and thaw and repelletted at 100 000 *g* for 1 h. MVs were resuspended in annexin-V, biotin conjugated for 30 min, washed and repelleted. For biochemical fractionation of MVs, total lipids were extracted through the method previously described (Riboni *et al*, 2000) with 2:1 (by volume) of chloroform and methanol. The lipid fraction was evaporated under a nitrogen stream, dried for 1 h at 50°C and resuspended in PBS at 40°C in order to obtain multilamellar vesicles. Small unilamellar vesicles were obtained by sonicating multilamellar vesicles, following the procedure of Barenholz *et al* (1977).

Electrophysiological recordings

Whole-cell voltage clamp recordings were obtained with an Axopatch 200-B amplifier and pCLAMP software, mEPSCs were recorded at −70 mV in the presence of 1 μM TTX at room temperature (20–25°C) and analysed using Clampfit software. All experiments were performed in 1.7×10^5 neurons/coverslip, cultured for 12–14 days. The mean mEPSC frequency was ∼1 Hz. Paired recordings were made from low-density cultures with a 1-ms depolarization to +30 mV. Short-term plasticity was measured at an interstimulus of 50 ms. For RRP measurements, hypertonic solution containing 6 mM sucrose was infused with a puffer pipette for 4 s. Currents were filtered at 2 kHz and sampled above 5 kHz. External control solutions contained 125 mM NaCl, 5 mM KCl, 1.2 mM $MgSO_4$, 1.2 mM KH_2PO, 2 mM $CaCl_2$, 6 mM D-glucose, and 25 mM HEPES/NaOH, pH 7.4. Recording pipettes were fabricated from capillary glass using a two-stage puller (Narishige, Japan) and had tip resistances of 3–5 MΩ when filled with the intracellular solution of the following composition, 130 mM potassium gluconate, 10 mM KCl, 1 mM EGTA, 10 mM HEPES, 2 mM $MgCl_2$, 4 mM MgATP, 0.3 mM Tris-GTP. Series resistance was monitored during experiments, and recordings with changes over 20% control during experiments were rejected.

MVs injection and VEP recordings

Recordings were conducted in P26–P30 rats as described previously (Caleo *et al*, 2007; Restani *et al*, 2009). Briefly, animals were anaesthetized with urethane (20% solution in saline, Sigma; 0.6 ml/100 g body weight) and placed in a stereotaxic apparatus. Body temperature during the experiments was constantly monitored with a rectal probe and maintained at 37°C with a heating blanket. A glass micropipette (2 MΩ) filled with NaCl (3 M) was mounted on a three axis motorized micromanipulator and inserted into the binocular portion of visual cortex. VEPs and single units (6–8 cells) were recorded from a single penetration in one hemisphere. After this baseline recording, an injection pipette held by a second micromanipulator was used to deliver saline or MVs (derived from 2×10^6 N9 cells dissolved in 1 μl of sterile saline) in the vicinity (<1 mm) of the recording electrode. After a delay of 20 min, we started to record VEPs and single units again along the same penetration. Care was taken to record at the same coordinates before and after injection in each animal. For extracellular recordings of spiking activity, visual stimuli were delivered to the contralateral eye and consisted of a computer-generated bar (contrast, 90%; thickness, 3°; speed, 28°/second) presented on a monitor (Sony, 40 × 30 cm; mean luminance 15 cd/m^2). Signals were amplified 25 000-fold, bandpass filtered (300–5000 Hz), and conveyed to a computer for storage and analysis. Action potentials were discriminated from background by a voltage threshold, that was set as 4.5 times the standard deviation of noise, as described (Caleo *et al*, 2007). RF sizes were determined from peristimulus time histograms (PSTHs; bin size = 33 ms) of the cell response to the stimulus, averaged over 20 consecutive stimulations as described (Caleo *et al*, 2007). For VEP recordings, the electrode was typically positioned at a depth of 100 μm within the cortex. Steady-state VEPs were recorded in response to reversal (4 Hz) of a horizontal sinusoidal grating (spatial frequency, 0.07 cycles/degree; contrast 0, 10, 20, 30, 90%), generated by computer on a display (Sony; 40 × 30 cm; mean luminance 15 cd/m^2) by a VSG card (Cambridge Research System). Signals were amplified (1000–2000-fold), bandpass filtered (0.1–500 Hz), and fed to a computer for storage and analysis. At least 100 events were averaged in synchrony with the stimulus contrast reversal. VEP amplitude was quantified by measuring the amplitude of the second harmonic of the Fourier transform computed from the recorded signal (Caleo *et al*, 2003). The response to a blank stimulus (0% contrast) was frequently recorded to estimate noise. The response amplitude was expressed as the ratio between the VEP amplitude at a given contrast and the VEP amplitude at 90% contrast before MVs (or saline) delivery.

Immunocytochemical assay

Neurons were incubated with antibodies against the intravesicular domain of synaptotagmin I (Syt-ECTO; SYSY) in 50 mM KCl solution for 4 min, washed, fixed, and stained with a secondary antibody and for vesicular glutamate transporter-1 (vGlut1). Images were acquired using a Meta confocal microscope and analysed by Image J software. vGlut1-positive recycling synapses were revealed by generating a binary mask of Syt-ECTO/vGlut1 double-positive images. Total count of Syt-ECTO-positive synapses was normalized to the total count of the corresponding vGlut1 staining. Synapses were scored as positive for Syt-ECTO Ab internalization when the fluorescence intensity was at least 2.5-fold higher as compared with that of cultures exposed only to secondary antibodies. Increase in synaptic vesicle recycling rate results in more efficient Syt-ECTO Ab internalization, bringing subthreshold synapses above threshold levels (Bacci *et al*, 2001).

Assessment of MVs rupture: flow cytometry analysis of CMFDA-labelled MVs and IL-1β ELISA. In all, 10^6 cells primary microglia were loaded with the fluorescent dye CMFDA (10 μM) for 1 h, washed and exposed to BzATP. MVs shed into the supernatant were either pelletted at 10 000 *g* for 30 min or subjected to freeze and

thaw before being isolated by centrifugation. Intact and freeze and thaw MVs derived from CMFDA-labelled microglia were then diluted in PBS buffer and MVs were acquired on a Canto II HTS flow cytometer using FCS 3 software (Becton Dickinson). A gate was established on size using beads of 0.5–2 μm. At least 5×10^4 events were analysed. Alternatively, intact and freeze and thaw MVs derived from 10^6 N9 microglia, primed for 6 h with 100 ng/ml LPS, were resuspended in 100 μl of saline and IL-1β released into the saline from MVs was quantified by a mouse IL-1β ELISA kit (Pierce Endogen, Italy), following the manufacturing procedure.

[Sph-3H] SM metabolism

In all, 10^6 neurons at 7DIV were maintained 1 h in neuronal medium without B27 supplement. Stock solutions of [Sph-3H]SM in absolute ethanol were prepared and added to fresh medium. The final concentration of ethanol never exceeded 0.1% (v/v). The cells were pulsed 1 h with [Sph-3H]SM (0.11 μCi/ml) followed by 1 h chase, in neuron conditioned medium, with or without MVs. At the end of chase, the cells were washed twice with PBS at 4°C and harvested, and total lipids extracted and processed as previously described (Riboni *et al*, 2000). The methanolized organic phase was analysed by HPTLC using different solvent systems: chloroform/methanol/water (55:20:3 by volume) and chloroform/methanol/acetone/acetic acid/water (75:15:30:15:7.5 by volume). Digital autoradiography of HPTLC plates was performed with Beta-Imager 2000 (Biospace, France), and the radioactivity associated with individual lipids measured using the software provided with the instrument. The 3H-labelled sphingolipids were recognized and identified as described previously (Riboni *et al*, 2000).

Liposomes

Small unilamellar vesicles of bovine brain PC, bovine brain PS, bovine brain SM, and cholesterol (60:10:10:20, molar ratio) were dissolved in chloroform. The lipid mixtures were evaporated under a nitrogen stream, dried for 1 h at 50°C and resuspended in PBS at 40°C in order to obtain multilamellar vesicles. Small unilamellar vesicles were obtained by sonicating multilamellar vesicles, following the procedure of Barenholz *et al* (1977).

Reagents

BzATP, LPS, annexin-V, NOE, and A-SMase were from Sigma-Aldrich. SKI-1 was from Echelon Biosciences. CellTracker green CMFDA was from Molecular Probes. TTX was from Tocris. PC, PS, cholesterol, and SM were from Sigma-Aldrich. Sph and S-1P were from Biomol. [Sph-3H]sphingomyelin (3H SM) was obtained as previously described (Riboni *et al*, 2000). TNF-α and IL-1β neutralizing Abs were from R&D.

Statistical analysis

Data are presented as mean ± s.e. from the indicated number of experiments. Statistical significance was evaluated using the indicated test. The differences were considered to be significant if $P<0.05$ and are indicated by an asterisk; those at $P<0.01$ are indicated by double asterisks and those at $P<0.001$ are indicated by triple asterisks.

Supplementary data

Supplementary data are available at *The EMBO Journal* Online (http://www.embojournal.org).

Acknowledgements

We thank E Menna (CNR, Milan) and R Furlan (San Raffaele Hospital, Milan) for helpful discussion and A Bergami (San Raffaele Hospital, Milan) for flow cytometry measurements. This research has been supported by FISM 2010/R/39 to CV, Compagnia di San Paolo, 2008 2207 to MM and Associazione Italiana Ricerca sul Cancro (AIRC) to EC.

Author contributions: FA performed all patch-clamp recordings *in vitro* with the help of MG, analysed data and helped with *in-vivo* experiments. ET established cultured microglia, performed MV isolations and part of MV biochemical treatments with the help of LN. LR established cultured neurons and performed some biochemistry on MVs. MC performed and analysed *in-vivo* data and helped with data interpretation. CP analysed A-SMase activity of MVs. EC provided experimental tools. PG analysed sphingolipid metabolism and extracted lipid fraction from MVs. PV discussed the hypothesis and helped with data interpretation. MM discussed the hypothesis and helped to write the manuscript. CV designed the study and wrote the manuscript.

Conflict of interest

The authors declare that they have no conflict of interest.

References

Akira S, Takeda K (2004) Toll-like receptor signalling. *Nat Rev Immunol* **4:** 499–511

Al-Nedawi K, Meehan B, Micallef J, Lhotak V, May L, Guha A, Rak J (2008) Intercellular transfer of the oncogenic receptor EGFRvIII by microvesicles derived from tumour cells. *Nat Cell Biol* **10:** 619–624

Al-Nedawi K, Meehan B, Rak J (2009) Microvesicles: messengers and mediators of tumor progression. *Cell Cycle* **8:** 2014–2018

Bacci A, Coco S, Pravettoni E, Schenk U, Armano S, Frassoni C, Verderio C, De Camilli P, Matteoli M (2001) Chronic blockade of glutamate receptors enhances presynaptic release and downregulates the interaction between synaptophysin-synaptobrevin-vesicle-associated membrane protein 2. *J Neurosci* **21:** 6588–6596

Barenholz Y, Gibbes D, Litman BJ, Goll J, Thompson TE, Carlson RD (1977) A simple method for the preparation of homogeneous phospholipid vesicles. *Biochemistry* **16:** 2806–2810

Benali A, Weiler E, Benali Y, Dinse HR, Eysel UT (2008) Excitation and inhibition jointly regulate cortical reorganization in adult rats. *J Neurosci* **28:** 12284–12293

Bianco F, Colombo A, Saglietti L, Lecca D, Abbracchio MP, Matteoli M, Verderio C (2009a) Different properties of P2X(7) receptor in hippocampal and cortical astrocytes. *Purinergic Signal* **5:** 233–240

Bianco F, Perrotta C, Novellino L, Francolini M, Riganti L, Menna E, Saglietti L, Schuchman EH, Furlan R, Clementi E, Matteoli M, Verderio C (2009b) Acid sphingomyelinase activity triggers microparticle release from glial cells. *EMBO J* **28:** 1043–1054

Bianco F, Pravettoni E, Colombo A, Schenk U, Moller T, Matteoli M, Verderio C (2005) Astrocyte-derived ATP induces vesicle shedding and IL-1 beta release from microglia. *J Immunol* **174:** 7268–7277

Busche MA, Eichhoff G, Adelsberger H, Abramowski D, Wiederhold KH, Haass C, Staufenbiel M, Konnerth A, Garaschuk O (2008) Clusters of hyperactive neurons near amyloid plaques in a mouse model of Alzheimer's disease. *Science* **321:** 1686–1689

Caleo M, Medini P, von Bartheld CS, Maffei L (2003) Provision of brain-derived neurotrophic factor via anterograde transport from the eye preserves the physiological responses of axotomized geniculate neurons. *J Neurosci* **23:** 287–293

Caleo M, Restani L, Gianfranceschi L, Costantin L, Rossi C, Rossetto O, Montecucco C, Maffei L (2007) Transient synaptic silencing of developing striate cortex has persistent effects on visual function and plasticity. *J Neurosci* **27:** 4530–4540

Camoletto PG, Vara H, Morando L, Connell E, Marletto FP, Giustetto M, Sassoe-Pognetto M, Van Veldhoven PP, Ledesma MD (2009) Synaptic vesicle docking: sphingosine regulates syntaxin1 interaction with Munc18. *PLoS One* **4:** e5310

Centonze D, Muzio L, Rossi S, Cavasinni F, De Chiara V, Bergami A, Musella A, D'Amelio M, Cavallucci V, Martorana A, Bergamaschi A, Cencioni MT, Diamantini A, Butti E, Comi G, Bernardi G, Cecconi F, Battistini L, Furlan R, Martino G (2009) Inflammation triggers synaptic alteration and degeneration in experimental autoimmune encephalomyelitis. *J Neurosci* **29:** 3442–3452

Cocucci E, Racchetti G, Meldolesi J (2009) Shedding microvesicles: artefacts no more. *Trends Cell Biol* **19:** 43–51

Darios F, Wasser C, Shakirzyanova A, Giniatullin A, Goodman K, Munoz-Bravo JL, Raingo J, Jorgacevski J, Kreft M, Zorec R, Rosa JM, Gandia L, Gutierrez LM, Binz T, Giniatullin R, Kavalali ET,

Davletov B (2009) Sphingosine facilitates SNARE complex assembly and activates synaptic vesicle exocytosis. *Neuron* **62:** 683–694

Davletov B, Montecucco C (2010) Lipid function at synapses. *Curr Opin Neurobiol* **20:** 543–549

De Felice FG, Velasco PT, Lambert MP, Viola K, Fernandez SJ, Ferreira ST, Klein WL (2007) Abeta oligomers induce neuronal oxidative stress through an N-methyl-D-aspartate receptor dependent mechanism that is blocked by the Alzheimer drug memantine. *J Biol Chem* **282:** 11590–11601

Del Conde I, Shrimpton CN, Thiagarajan P, Lopez JA (2005) Tissue-factor-bearing microvesicles arise from lipid rafts and fuse with activated platelets to initiate coagulation. *Blood* **106:** 1604–1611

Graeber MB (2010) Changing face of microglia. *Science* **330:** 783–788

Graner MW, Alzate O, Dechkovskaia AM, Keene JD, Sampson JH, Mitchell DA, Bigner DD (2009) Proteomic and immunologic analyses of brain tumor exosomes. *FASEB J* **23:** 1541–1557

Horinouchi K, Erlich S, Perl DP, Ferlinz K, Bisgaier CL, Sandhoff K, Desnick RJ, Stewart CL, Schuchman EH (1995) Acid sphingomyelinase deficient mice: a model of types A and B Niemann-Pick disease. *Nat Genet* **10:** 288–293

Jabs R, Matthias K, Grote A, Grauer M, Seifert G, Steinhäuser C (2007) Lack of P2X receptor mediated currents in astrocytes and GluR type glial cells of the hippocampal CA1 region. *Glia* **55:** 1648–1655

Kajimoto T, Okada T, Yu H, Goparaju SK, Jahangeer S, Nakamura S (2007) Involvement of sphingosine-1-phosphate in glutamate secretion in hippocampal neurons. *Mol Cell Biol* **27:** 3429–3440

Kanno T, Nishizaki T, Proia RL, Kajimoto T, Jahangeer S, Okada T, Nakamura S (2010) Regulation of synaptic strength by sphingosine 1-phosphate in the hippocampus. *Neuroscience* **171:** 973–980

Kosaka N, Iguchi H, Yoshioka Y, Takeshita F, Matsuki Y, Ochiya T (2010) Secretory mechanisms and intercellular transfer of microRNAs in living cells. *J Biol Chem* **285:** 17442–17452

Ledesma MD, Prinetti A, Sonnino S, Schuchman EH (2011) Brain pathology in Niemann Pick disease type A: insights from the acid sphingomyelinase knockout mice. *J Neurochem* **116:** 779–788

Liu BH, Li P, Sun YJ, Li YT, Zhang LI, Tao HW (2010) Intervening inhibition underlies simple cell receptive field structure in visual cortex. *Nat Neurosci* **13:** 89–96

Matteoli M, Takei K, Perin MS, Sudhof TC, De Camilli P (1992) Exo-endocytotic recycling of synaptic vesicles in developing processes of cultured hippocampal neurons. *J Cell Biol* **117:** 849–861

Norman E, Cutler RG, Flannery R, Wang Y, Mattson MP (2010) Plasma membrane sphingomyelin hydrolysis increases hippocampal neuron excitability by sphingosine-1-phosphate mediated mechanisms. *J Neurochem* **114:** 430–439

Okada T, Kajimoto T, Jahangeer S, Nakamura S (2009) Sphingosine kinase/sphingosine 1-phosphate signalling in central nervous system. *Cell Signal* **21:** 7–13

Olah M, Biber K, Vinet J, Boddeke HW (2011) Microglia phenotype diversity. *CNS Neurol Disord Drug Targets* **10:** 108–118

Porciatti V, Pizzorusso T, Maffei L (1999) The visual physiology of the wild type mouse determined with pattern VEPs. *Vision Res* **39:** 3071–3081

Proia P, Schiera G, Mineo M, Ingrassia AM, Santoro G, Savettieri G, Di Liegro I (2008) Astrocytes shed extracellular vesicles that contain fibroblast growth factor-2 and vascular endothelial growth factor. *Int J Mol Med* **21:** 63–67

Qu Y, Ramachandra L, Mohr S, Franchi L, Harding CV, Nunez G, Dubyak GR (2009) P2X7 receptor-stimulated secretion of MHC class II-containing exosomes requires the ASC/NLRP3 inflammasome but is independent of caspase-1. *J Immunol* **182:** 5052–5062

Ransohoff RM, Cardona AE (2010) The myeloid cells of the central nervous system parenchyma. *Nature* **468:** 253–262

Ratajczak J, Wysoczynski M, Hayek F, Janowska-Wieczorek A, Ratajczak MZ (2006) Membrane derived microvesicles: important and underappreciated mediators of cell-to-cell communication. *Leukemia* **20:** 1487–1495

Restani L, Cerri C, Pietrasanta M, Gianfranceschi L, Maffei L, Caleo M (2009) Functional masking of deprived eye responses by callosal input during ocular dominance plasticity. *Neuron* **64:** 707–718

Riboni L, Viani P, Tettamanti G (2000) Estimating sphingolipid metabolism and trafficking in cultured cells using radiolabeled compounds. *Methods Enzymol* **311:** 656–682

Rosenmund C, Stevens CF (1996) Definition of the readily releasable pool of vesicles at hippocampal synapses. *Neuron* **16:** 1197–1207

Roumier A, Bechade C, Poncer JC, Smalla KH, Tomasello E, Vivier E, Gundelfinger ED, Triller A, Bessis A (2004) Impaired synaptic function in the microglial KARAP/DAP12-deficient mouse. *J Neurosci* **24:** 11421–11428

Sadallah S, Eken C, Schifferli JA (2011) Ectosomes as modulators of inflammation and immunity. *Clin Exp Immunol* **163:** 26–32

Sarkar A, Mitra S, Mehta S, Raices R, Wewers MD (2009) Monocyte derived microvesicles deliver a cell death message via encapsulated caspase-1. *PLoS One* **4:** e7140

Sbai O, Ould-Yahoui A, Ferhat L, Gueye Y, Bernard A, Charrat E, Mehanna A, Risso JJ, Chauvin JP, Fenouillet E, Rivera S, Khrestchatisky M (2010) Differential vesicular distribution and trafficking of MMP-2, MMP-9, and their inhibitors in astrocytes. *Glia* **58:** 344–366

Sims PJ, Wiedmer T (2001) Unraveling the mysteries of phospholipid scrambling. *Thromb Haemost* **86:** 266–275

Skog J, Wurdinger T, van Rijn S, Meijer DH, Gainche L, Sena-Esteves M, Curry Jr WT, Carter BS, Krichevsky AM, Breakefield XO (2008) Glioblastoma microvesicles transport RNA and proteins that promote tumour growth and provide diagnostic biomarkers. *Nat Cell Biol* **10:** 1470–1476

Strelow A, Bernardo K, Adam-Klages S, Linke T, Sandhoff K, Kronke M, Adam D (2000) Overexpression of acid ceramidase protects from tumor necrosis factor-induced cell death. *J Exp Med* **192:** 601–612

Thomas LM, Salter RD (2010) Activation of macrophages by P2X7-induced microvesicles from myeloid cells is mediated by phospholipids and is partially dependent on TLR4. *J Immunol* **185:** 3740–3749

Trajkovic K, Hsu C, Chiantia S, Rajendran L, Wenzel D, Wieland F, Schwille P, Brugger B, Simons M (2008) Ceramide triggers budding of exosome vesicles into multivesicular endosomes. *Science* **319:** 1244–1247

van der Vos KE, Balaj L, Skog J, Breakefield XO (2011) Brain tumor microvesicles: insights into intercellular communication in the nervous system. *Cell Mol Neurobiol* **31:** 949–959

Verderio C, Matteoli M (2001) ATP mediates calcium signaling between astrocytes and microglial cells: modulation by IFN-gamma. *J Immunol* **166:** 6383–6391

Vezzani A, Ravizza T, Balosso S, Aronica E (2008) Glia as a source of cytokines: implications for neuronal excitability and survival. *Epilepsia* **49**(Suppl 2)**:** 24–32

Viviani B, Gardoni F, Marinovich M (2007) Cytokines and neuronal ion channels in health and disease. *Int Rev Neurobiol* **82:** 247–263

Wake H, Moorhouse AJ, Jinno S, Kohsaka S, Nabekura J (2009) Resting microglia directly monitor the functional state of synapses *in vivo* and determine the fate of ischemic terminals. *J Neurosci* **29:** 3974–3980

Zwaal RF, Schroit AJ (1997) Pathophysiologic implications of membrane phospholipid asymmetry in blood cells. *Blood* **89:** 1121–1132

